A Rayleigh-Ritz method based on improved Fourier series for vibration analysis of cylindrical shell coupled with elastic beams

Zhang Runze[1]; Cao Yipeng[1]; Li liaoyuan[1]

[1] College of Power and Energy Engineering, Harbin Engineering University, Harbin, P.R. China

ABSTRACT

A finite circular cylindrical shell model coupled with elastic beams is built in this paper. The beam-shell structure is connected with linear springs and rotational springs. Considering different structural coupling conditions, the Rayleigh-Ritz approach based on improved Fourier series method is employed to analyze the free vibration properties of the calculation model. The improved Fourier series method is used to describe the displacements of the coupling structure, while the Rayleigh-Ritz method is utilized to solve the coefficients. The important advantage of this approach is that it can be universally applied to the coupling structure with a variety of different boundary and coupling conditions. The results are verified by the finite element method. It's shown that the proposed approach is a convenient, efficient and accurate one for determining the modal behavior of such a complex structure system.

Keywords: beam-shell structure, coupling conditions, Rayleigh-Ritz approach, improved Fourier series method

1. INTRODUCTION

The vibration studies of a finite circular cylindrical shell model coupled with elastic beams have separately received a great deal of attention. When the two structures are coupled together the behavior of the resulting structure is more complex and, consequently, there is less literature available on the topic. However, the study of these combined structures is of great importance in many engineering applications, such as in the design of aeronautical or space structures, submarine structure and industrial vessels. This paper investigates the free vibration characteristics of one variant of these structures.

In recent years, many efforts have been made on vibration analysis with relatively simple structures such as beams and cylindrical shells. As far as elastic beams are concerned, a large body of literature exists. Hsien-Yuan Lin[1,2] used numerical assembly method to study the free and forced vibration of multi-span beam with various intermediate unit (including the middle support, lumped mass, mass spring system, etc.). W.L.Li[3,4,5] proposed an improved Fourier series method to establish the multi-span beam model with the elastic support and calculated the natural characteristics and dynamic response under moving load. Cao Yipeng[6] used the Rayleigh-Ritz method based on an improved Fourier series to solve the coupled three-dimensional beam. For circular cylindrical shells, Zhou Haijun[7] solved the free vibration of cylindrical shell under elastic support boundary condition with fluctuation analysis method, in which he analyzed the influence of boundary stiffness to natural frequency of cylindrical shell. Dai Lu[8] applied exact Fourier series as displacement admissible function and substituted it into governing equation to solve the free vibration characteristic of cylindrical shell under any boundary conditions, of which the results show that the accuracy is higher. As to combine shell-plate structures, less literature is available. Missaoui[9] established variation equation of coupled structure by simulating the coupling system via introducing spring. Guo[10,11] focused on the influence of internal structure to structure vibration. He applied the displacement admittance theory to obtain the effect of force and moment between plate and shell, thus he made great contribution to the influence of coupling between internal and shell structure.

[1] runze_wuyang@yahoo.com

2. Theoretical model

2.1 Description of the model

The co-ordinate system and various diagrams illustrating the parameters used in the model are shown in Figure 1. The structure consists of a finite circular cylindrical shell coupled with elastic beams at middle of the shell. The shell has a length L and is assumed to be thin; that is, its wall thickness h is much smaller than its radius R. Therefore, the conventional assumptions of flűgge's shell equation are adopted. The shell displacement is represented by U, V and W, which are, respectively, axial displacement, tangential displacement and radial displacement.

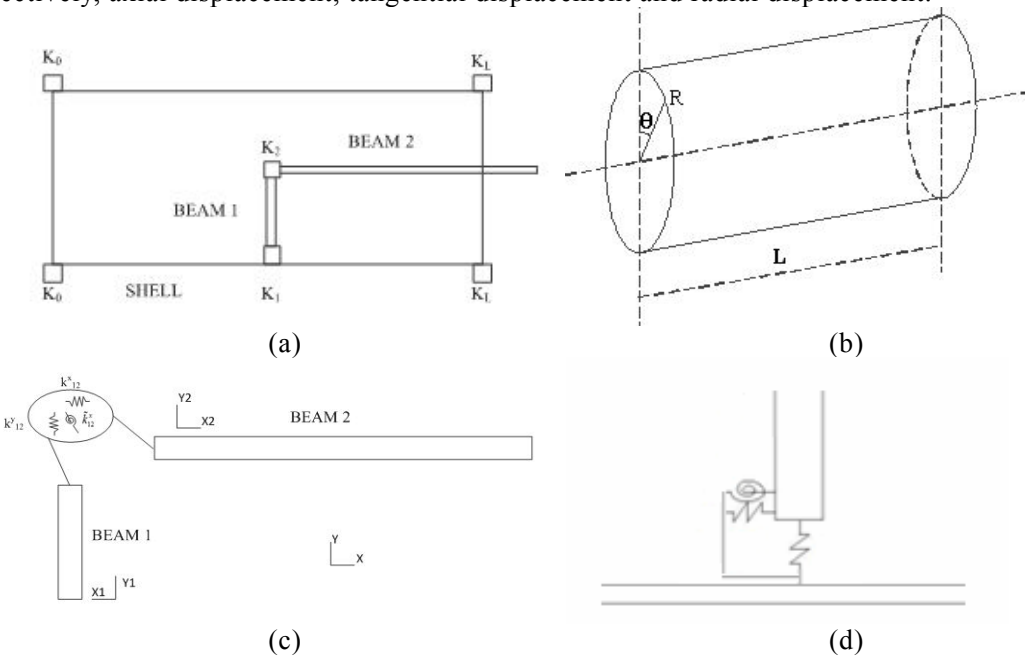

Figure 1- Structure diagram of the structure : (a) beam-shell structure; (b) cylindrical shell; (c) beam; (d) beam-shell interface at x=L/2

For the beam, the beam i has a length L_{Bi}, and its cross-section is square, the length of the square is b which is much smaller than the beams' length, therefore, It is assumed that beam is Euler Bernoulli beam. The beam displacement is represented by U_i, $W_{i,y}$, $W_{i,z}$ and θ_i, which are respectively, axial, vertical and horizontal displacement and rotation angle around x-axis of the ith beam. The beam-shell joint at x=L/2 can be seen in figures 1(d). Boundary and coupling of the beam-shell structure are constrained by linear springs and rotational springs as shown in Figure 1. By changing the stiffness of springs from zero to infinite, it is easy to obtain the clamped, simply supported and free boundary conditions. The form of springs is shown in Table 1.

Table 1-The form of springs

K_i	axial-direction spring	tangential -direction spring	radial -direction spring	torsion spring
K_0	k_1	k_2	k_3	k_4
K_L	k_5	k_6	k_7	k_8

K_i	x-direction spring	y-direction spring	z-direction spring	around x-axis torsion spring	around y-axis torsion spring	around z-axis torsion spring
K_1	k_c^x	k_c^y	k_c^z	$\tilde{k}_c^x$	$\tilde{k}_c^y$	$\tilde{k}_c^z$
K_2	k_{ij}^x	k_{ij}^y	k_{ij}^z	$\tilde{k}_{ij}^x$	$\tilde{k}_{ij}^y$	$\tilde{k}_{ij}^z$

2.2 Series representations of the displacement functions

2.2.1 Series representations of the displacement functions

Axial, tangential and radial displacement can be respectively represented as follows:

$$\begin{aligned} U(x,\theta,t) &= u(x,\theta)e^{jwt} \\ V(x,\theta,t) &= v(x,\theta)e^{jwt} \\ W(x,\theta,t) &= w(x,\theta)e^{jwt} \end{aligned} \tag{1}$$

Where, ω is the angular frequency. The displacement admissible function of cylindrical shell can be represented as improved Fourier series form. The improved Fourier series expansion can be written as:

$$\begin{aligned} u(x,\theta) &= \sum_{m=0}^{\infty}\sum_{n=0}^{\infty} a^{u}_{mn}\cos(\lambda_m x)\cos n\theta + \sum_{l=1}^{2}\sum_{n=0}^{\infty}\alpha^{u}_{ln}\xi_l(x)\cos n\theta \\ v(x,\theta) &= \sum_{m=0}^{\infty}\sum_{n=0}^{\infty} a^{v}_{mn}\cos(\lambda_m x)\sin n\theta + \sum_{l=1}^{2}\sum_{n=0}^{\infty}\alpha^{v}_{ln}\xi_l(x)\sin n\theta \\ w(x,\theta) &= \sum_{m=0}^{\infty}\sum_{n=0}^{\infty} a^{w}_{mn}\cos(\lambda_m x)\cos n\theta + \sum_{l=1}^{4}\sum_{n=0}^{\infty}\alpha^{w}_{ln}\xi_l(x)\cos n\theta \end{aligned} \tag{2}$$

Where, ξ is the additional auxiliary function to make the boundary continuous. They are continuous and derivable functions which satisfy the boundary conditions. Auxiliary polynomial function form is given here:

$$\begin{Bmatrix} \xi_1(x) \\ \xi_2(x) \\ \xi_3(x) \\ \xi_4(x) \end{Bmatrix} = \begin{Bmatrix} \dfrac{6Lx-2L^2-3x^2}{6L} \\ \dfrac{3x^2-L^2}{6L} \\ \dfrac{-15x^4+60Lx^3-60L^2x^2+8L^4}{360L} \\ \dfrac{15x^4-30L^2x^2+7L^4}{360L} \end{Bmatrix} \tag{3}$$

2.2.2 Series representations of the displacement functions

Axial, vertical and horizontal displacement and rotation angle around x-axis of the *i*th beam can be respectively represented as follows:

$$\begin{aligned} U_i(x,t) &= u_i(x)\mathrm{e}^{\mathrm{j}\omega t} \qquad W_{i,y}(x,t) = w_{i,y}(x)\mathrm{e}^{\mathrm{j}\omega t} \\ W_{i,z}(x,t) &= w_{i,z}(x)\mathrm{e}^{\mathrm{j}\omega t} \qquad \Theta_i(x,t) = \theta_i(x)\mathrm{e}^{\mathrm{j}\omega t} \end{aligned} \tag{4}$$

Where, the subscript *i* is on behalf of the beam *i*. ω is the angular frequency. According to the literature[4], the displacement admissible function of beam *i* can be represented as improved Fourier series form. ϕ represent u_i, $w_{i,y}$, $w_{i,z}$ or θ_i the improved Fourier series expansion can be written as:

$$\begin{aligned} u_i(x) &= \sum_{m=0}^{M} A^{m}_{u_i}\cos(\lambda_{im}x) + \sum_{l=1}^{2}\alpha_{u_i}\cdot\xi^{T}_{l}(x) \\ w_{i,y}(x) &= \sum_{m=0}^{M} A^{m}_{w_{i,y}}\cos(\lambda_{im}x) + \sum_{l=1}^{4}\alpha_{w_{i,y}}\cdot\xi^{T}_{l}(x) \\ w_{i,z}(x) &= \sum_{m=0}^{M} A^{m}_{w_{i,z}}\cos(\lambda_{im}x) + \sum_{l=1}^{4}\alpha_{w_{i,z}}\cdot\xi^{T}_{l}(x) \\ \theta_i(x) &= \sum_{m=0}^{M} A^{m}_{\theta_i}\cos(\lambda_{im}x) + \sum_{l=1}^{2}\alpha_{\theta_i}\cdot\xi^{T}_{l}(x) \end{aligned} \tag{5}$$

2.3 Series representations of the displacement functions

According to the coupling beam system shown in Figure 1, the Lagrange function can be expressed as:

$$\mathbf{L}_C = \mathbf{V}_S - \mathbf{T}_S - \mathbf{Q}_S + \mathbf{V}_B - \mathbf{T}_B - \mathbf{Q}_B + \mathbf{V}_{\mathbf{Bc}} + \mathbf{V}_c \tag{6}$$

Where **Vs** and $\mathbf{V_B}$ are respectively, the potential energy of the beam-shell structure, including their strain energy and the potential energy stored in the boundary spring and the potential energy associated with the coupling springs. $\mathbf{T_S}$ and $\mathbf{T_B}$ are their kinetic energy. $\mathbf{Q_S}$ and $\mathbf{Q_B}$ are the work done by external forces. $\mathbf{V_C}$ represents the potential energy stored in the coupling springs between the beam and cylindrical shell. These terms are

$$\begin{aligned}\mathbf{V_S} = &\frac{Eh}{2\left(1-\mu^2\right)}\int_0^{2\pi}\int_0^{l}\left[\frac{\partial U}{\partial x}+\frac{1}{R}\left(\frac{\partial V}{\partial \theta}+W\right)\right]^2 Rdxd\theta \\ &-\frac{Eh}{2\left(1-\mu^2\right)}\int_0^{2\pi}\int_0^{l}\frac{2\left(1-\mu\right)}{R}\left[\frac{\partial U}{\partial x}\left(\frac{\partial V}{\partial \theta}+W\right)\right]Rdxd\theta \\ &+\frac{Eh}{2\left(1-\mu^2\right)}\int_0^{2\pi}\int_0^{l}\frac{\left(1-\mu\right)}{2}\left[\frac{1}{R}\frac{\partial U}{\partial \theta}+\frac{\partial V}{\partial x}\right]^2 Rdxd\theta \\ &+\frac{Eh}{2\left(1-\mu^2\right)}\int_0^{2\pi}\int_0^{l}\frac{h^2}{12}\left[\frac{\partial^2 W}{\partial x^2}+\frac{1}{R^2}\left(\frac{\partial^2 W}{\partial \theta^2}-\frac{\partial V}{\partial \theta}\right)\right]^2 Rdxd\theta \\ &-\frac{Eh}{2\left(1-\mu^2\right)}\int_0^{2\pi}\int_0^{l}\frac{h^2}{12}\frac{2\left(1-\mu\right)}{R^2}\left[\frac{\partial^2 W}{\partial x^2}\left(\frac{\partial^2 W}{\partial \theta^2}-\frac{\partial V}{\partial \theta}\right)\right]Rdxd\theta \\ &+\frac{Eh}{2\left(1-\mu^2\right)}\int_0^{2\pi}\int_0^{l}\frac{h^2}{12}\frac{2\left(1-\mu\right)}{R^2}\left[\frac{\partial^2 W}{\partial x\partial \theta}-\frac{\partial V}{2\partial x}\right]^2 Rdxd\theta \\ &+\frac{1}{2}\int_0^{2\pi}\left[k_1u^2+k_2v^2+k_3w^2+k_4\left(\frac{\partial W}{\partial x}\right)^2\right]_{x=0} Rd\theta \\ &+\frac{1}{2}\int_0^{2\pi}\left[k_5u^2+k_6v^2+k_7w^2+k_8\left(\frac{\partial W}{\partial x}\right)^2\right]_{x=l} Rd\theta \end{aligned} \tag{7}$$

$$\mathbf{T}_S = \frac{1}{2}\int_0^{L}\int_0^{2\pi}\rho h\left[\left(\frac{\partial U}{\partial t}\right)^2+\left(\frac{\partial V}{\partial t}\right)^2+\left(\frac{\partial W}{\partial t}\right)^2\right]Rd\theta dx \tag{8}$$

$$\mathbf{Q}_S = \int_0^{2\pi}\int_0^{l_S}\left(F_u\left(x,\theta,t\right)U+F_v\left(x,\theta,t\right)V+F_w\left(x,\theta,t\right)W+M_w\left(x,\theta,t\right)\frac{\partial W}{\partial x}\right)dxd\theta \tag{9}$$

$$\mathbf{V_B} = \frac{1}{2}\sum_{i=1}^{2}\int_0^{l_i}\left[E_{Bi}\left(S_i\left(\frac{\partial U_i}{\partial x}\right)^2+I_{i,z}\left(\frac{\partial^2 W_{i,y}}{\partial x^2}\right)^2+I_{i,y}\left(\frac{\partial^2 W_{i,z}}{\partial x^2}\right)^2\right)+\frac{1}{2}G_iI_p\left(\frac{\partial \Theta_i}{\partial x}\right)^2\right] \tag{10}$$

$$\mathrm{T}_B = \frac{1}{2}\sum_{i=1}^{2}\int_0^{l_i}(\rho_{Bi}S_i\dot{U}_i^2+\rho_{Bi}S_i\dot{W}_{i,y}^2+\rho_{Bi}S_i\dot{W}_{i,z}^2+J_i\dot{\Theta}_i^2)dx \tag{11}$$

$$\begin{aligned}\mathbf{Q_B} = &\sum_{i=1}^{2}\int_0^{l_i}F_{U_i}(x,t)U_idx+\sum_{i=1}^{2}\int_0^{l_i}F_{W_{i,y}}(x,t)W_{i,y}dx+\sum_{i=1}^{2}\int_0^{l_i}F_{W_{i,z}}(x,t)W_{i,z}dx \\ &+\sum_{i=1}^{2}\int_0^{l_i}M_{\Theta_i}(x,t)\Theta_idx+\sum_{i=1}^{2}\int_0^{l_i}M_{W_{i,y}}(x,t)\frac{\partial W_{i,y}}{\partial x}dx+\sum_{i=1}^{2}\int_0^{l_i}M_{W_{i,z}}(x,t)\frac{\partial W_{i,z}}{\partial x}dx\end{aligned} \tag{12}$$

$$\begin{aligned}\mathbf{V_{12}} = &\frac{1}{2}k_{12}^{x}\left(W_{1,y}\big|_{x=l_1}+U_2\big|_{x=0}\right)^2+\frac{1}{2}k_{12}^{y}\left(U_1\big|_{x=l_1}-W_{2,y}\big|_{x=0}\right)^2+\frac{1}{2}k_{12}^{z}\left(W_{1,z}\big|_{x=l_1}-W_{2,z}\big|_{x=0}\right)^2 \\ &+\frac{1}{2}\tilde{k}_{12}^{x}\left(-\frac{\partial W_{1,z}}{\partial x}\bigg|_{x=l_1}+\Theta_2\big|_{x=0}\right)^2+\frac{1}{2}\tilde{k}_{12}^{y}\left(\Theta_1\big|_{x=l_1}-\frac{\partial W_{2,z}}{\partial x}\bigg|_{x=0}\right)^2+\frac{1}{2}\tilde{k}_{12}^{z}\left(\frac{\partial W_{1,y}}{\partial x}\bigg|_{x=l_1}-\frac{\partial W_{2,y}}{\partial x}\bigg|_{x=0}\right)^2\end{aligned} \tag{13}$$

$$\mathbf{V}_C = \frac{1}{2}k_c^x\left(U\big|_{x=R,\theta=0} + W_{1,y}\big|_{x=0}\right)^2 + \frac{1}{2}k_c^y\left(W\big|_{x=R,\theta=0} + U_1\big|_{x=0}\right)^2 + \frac{1}{2}k_c^z\left(V\big|_{x=R,\theta=0} - W_{1,z}\big|_{x=0}\right)^2 + \frac{1}{2}\tilde{k}_c^x\left(\left(\frac{V}{R} - \frac{\partial W}{R\partial\theta}\right)\Big|_{x=R,\theta=0} - \frac{\partial W_{1,z}}{\partial x}\Big|_{x=0}\right)^2 + \frac{1}{2}\tilde{k}_c^y\left(\left(\frac{\partial U}{R\partial\theta} + \frac{\partial V}{\partial x}\right)\Big|_{x=R,\theta=0} + \Theta_i\big|_{x=0}\right)^2 + \frac{1}{2}\tilde{k}_c^z\left(\frac{\partial W}{\partial x}\Big|_{x=R,\theta=0} + \frac{\partial W_{1,y}}{\partial x}\Big|_{x=0}\right)^2 \tag{14}$$

Where, ρ, μ and E are, respectively, the density, Poisson ratio, and Young's modulus of the shell material. The same symbols, with the subscript "B" added, are used to denote the equivalent characteristics of the beam material.

Substituting Eq. (2), Eq. (5) and Eqs.(7-14) into Eq.(6) and using Rayleigh-Ritz method to solve the Fourier and auxiliary polynomial coefficients. We can get the dynamic equilibrium equation of the coupling systems:

$$\left(\mathbf{K} - \boldsymbol{\omega}^2\mathbf{M}\right)\mathbf{C} = \mathbf{F} \tag{15}$$

Where the matrix **K** is the stiffness matrix of the system, the matrix **M** is the mass matrix of the system, the vector **C** is the coefficient vector, the vector **F** is the outside force vector

Once the stiffness and mass matrices are calculated, the responds of the coupling system caused by the external force can be calculated form Eq.(15). It is noteworthy that the modal properties can also be obtained from Eq. (15) by setting the external force vector to zero and solving a simple matrix eigenvalue problem. The modal frequencies for the structure are directly related to the eigenvalues. The actual modes, however, will have to be determined by substituting the eigenvectors into Eq.(1,2) and Eq.(4,5), because each of the eigenvector contains all the Fourier coefficients for the corresponding mode.

3. Discussion

As shown in Figure 1, The end of the shell is fixed onto the ground, corresponding spring stiffness are 1e10N/m. The left end of the vertical beam (Beam 1) is rigid connected with the shell, The left end of the vertical beam (Beam 1) is rigid connected with Horizontal beam (Beam 2) through the coupling springs. The coupling spring stiffness of the structure is 1e10N/m. The rest spring stiffness is 0.The properties for this beam-shell structure are summarized in Table 2. For model validation, this problem is solved using both the current method and the commercial finite element code, ANSYS.

Table 2-Parameters of each beam.

Parameter	Unit	Beam1	Beam2
L_B	m	0.24	0.8
S_B	m^2	0.0009	0.0009
I_B	m^4	6.75e-8	6.75e-8
E_B	Nm^{-2}	2.1e11	2.1e11
p_B	Kgm^{-3}	7800	7800

Table 3-Parameters of shell.

Parameter	Unit	Shell
R	m	0.247
h	m	0.006
E	N/m^2	2.1e11
ρ	kg/m^3	7785
μ		0.3

Table 4-Natural frequency comparison of coupling beam with vertical angle. f/Hz

Model	Current	FEA	error%
1	13.587	13.104	3.55
2	79.524	74.279	6.59
3	199.039	199.55	0.26
4	268.901	275.93	2.61
5	302.436	306.76	1.43
6	354.092	354.99	0.25
7	414.566	392.16	5.40
8	516.136	516.03	0.02
9	562.037	534.85	4.84
10	612.077	590.33	3.55
11	654.783	622.41	4.94
12	736.052	708.33	3.77
13	1158.369	1135.4	1.98

From Table 4, an excellent agreement is observed between these two sets of solutions with a maximum difference less than 5.4%. It illustrates the high precision and correctness of this method to solve natural frequencies of shafting. From Figure 2, it can be seen that the two sets of modes are essentially identical.

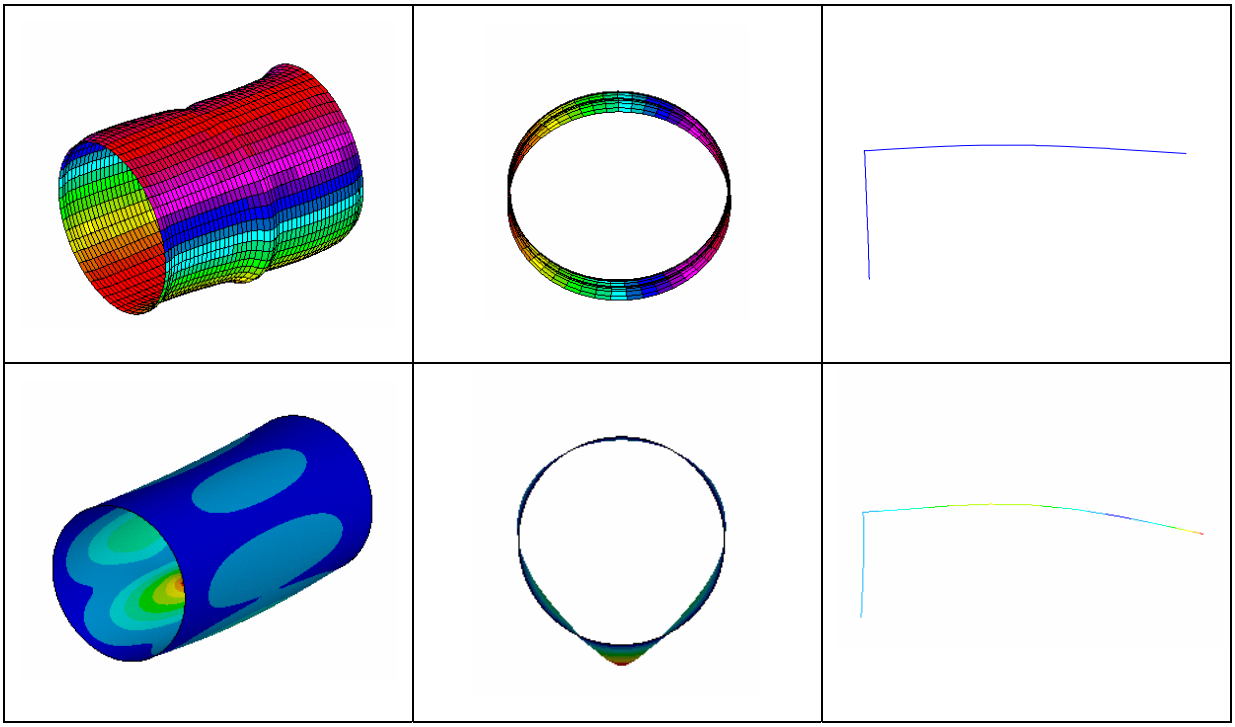

(a)

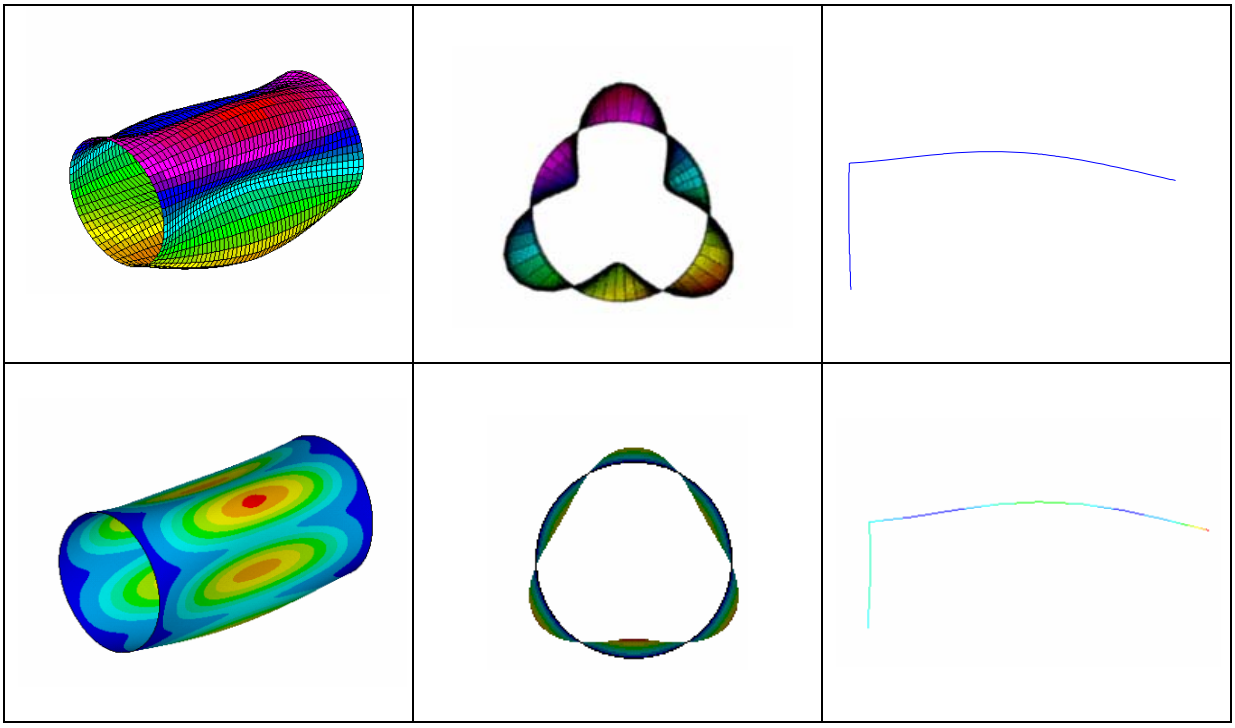

(b)

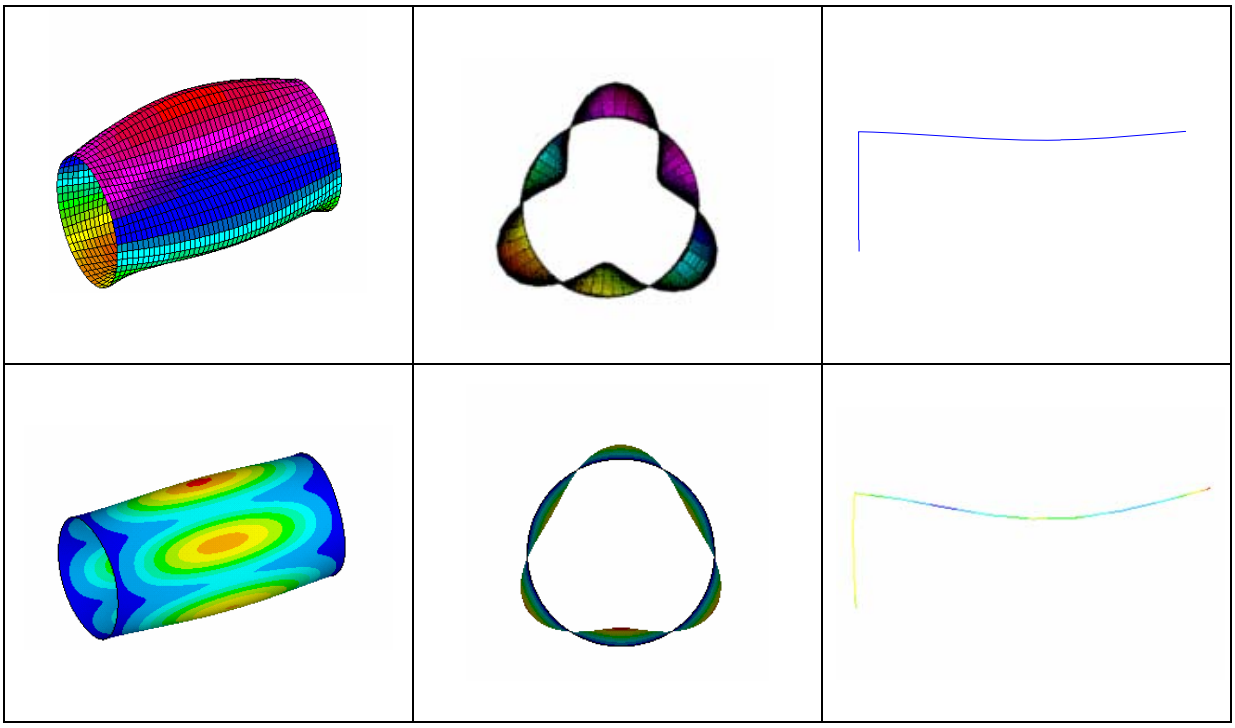

(c)

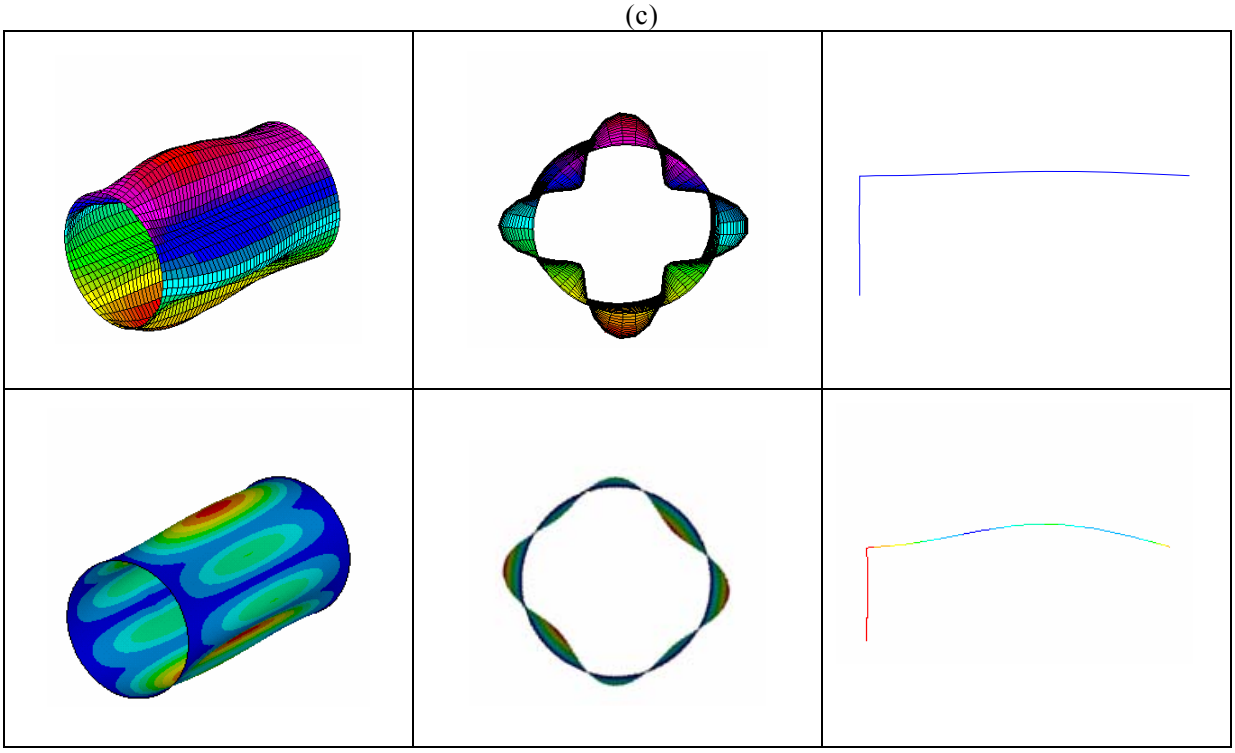

(d)

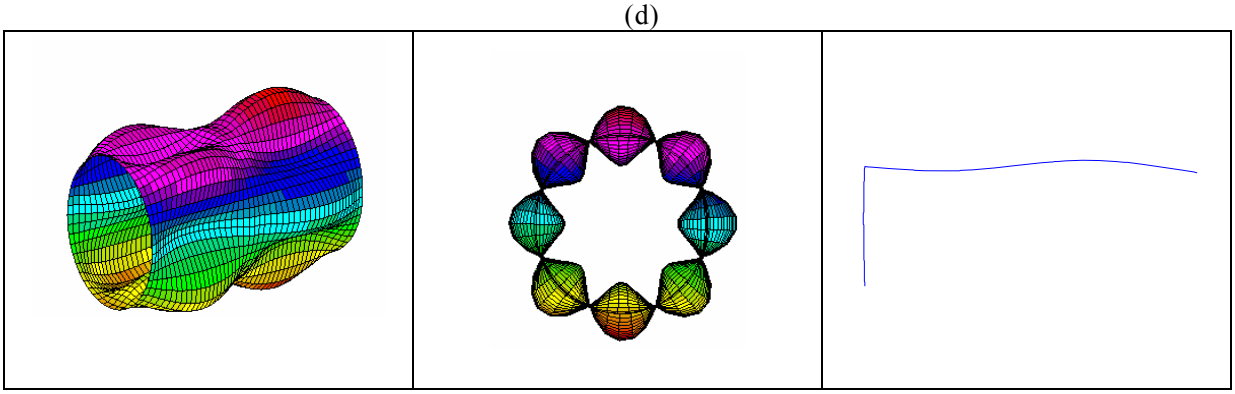

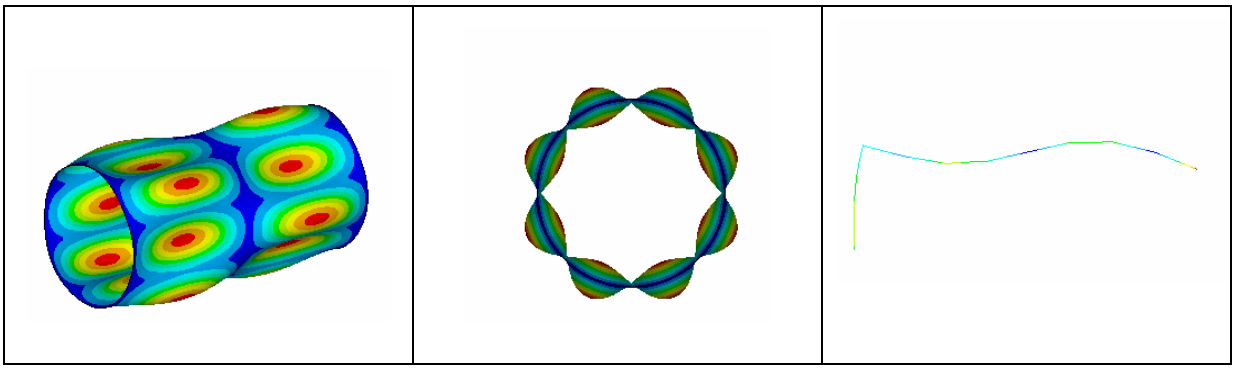

(e)

Figure 2 - Comparison of the shafting model shapes: (a) third; (b) fourth; (c) fifth; (d) seventh; (e) tenth;

From figure 2, modes which are obtained by the two methods are the same. Compare two kinds of method; the result matches very good, showing that the current method can be used to calculate the free vibration properties of the beam-shell structure.

4. CONCLUSIONS

A general analytical method has been developed for the Beam-Shell structure. Basing on the improved Fourier series method, the free and forced vibration characteristics are calculated. The results are compared with that by using finite element methods. The conclusions are as follows:

1. Based on the improved Fourier series method, displacement admissible function of beam and shell vibration is established. Rayleigh-Ritz method is utilized to solve the Fourier coefficient and auxiliary polynomial coefficients. The results show that the calculation program is simple and accurate which can be used to simulate the structure vibration properties with arbitrary boundary conditions considering different boundary spring stiffness.

2. The free and forced vibrations for propulsion shafting are investigated. The results indicate this method is accurate and reliable by comparing with the FEM, and can be used in the acquisition of shafting vibration.

ACKNOWLEDGEMENTS

The research is supported by the National Natural Science Foundation of China (No. 50909023). Their financial support is gratefully acknowledged.

REFERENCES

[1] Hsien-Yuan Lin, Free vibration analysis of a uniform multi-span beam carrying multiple spring mass systems, Journal of Sound and Vibration, 302(3), 442-456, (2007).
[2] Hsien-Yuan Lin, Dynamic analysis of a multi-span uniform beam carrying a number of various concentrated elements, Journal of Sound and Vibration, 309(1-2), 262-275, (2008).
[3] W.L.Li, Free vibrations of beams with general boundary conditions, Journal of Sound and Vibration, 237(4), 709-725(2000).
[4] W.L.Li, Vibrations of two beams elastically coupled together at an arbitrary angle, Acta Mechanica Solida Sinica, 25(1), 61-72, (2012).
[5] Hongan Xu, W.L.Li, Dynamic behavior of multi-span bridges under moving loads with focusing on the effect of the coupling conditions between spans , Journal of Sound and Vibration, 312(4-5),736-753, (2008).
[6] Cao Yipeng, Zhang Runze, The Rayleigh-Ritz method based on exact Fourier series for propulsion shafting system vibration analysis, ICSV 2014, Beijing China 2014.
[7] Haijun Zhou. Free vibrations of cylindrical shells with elastic-support boundary conditions [J].Applied Acoustics,2012 (73) :751–756
[8] Lu Dai, Tiejun Yang. An exact series solution for the vibration analysis of cylindrical shells with arbitrary boundary conditions [J]. Applied Acoustics, 2013(74):440-449.
[9] Missaoui,L.Cheng,M.J.Richard,Free and forced vibration of a cylindrical shell with a floor partion[J].Journal of Sound and Vibration,1996,190(1):1834-1843.
[10] Y.P.Guo,Acoustic radiation from cylindrical shells due to internal forcing[J].Journal of the Acoustical Society of America,1996,99(3):1495-1505
[11] Y.P.Guo, Acoustic acattering from cylindrical shells with deck-type internal plate at oblique incidence[J].Journal of the Acoustical Society of America,1996,99(5):2701-2713